Metal–Organic Network Assembly

Modular Assembly of Two-Dimensional Metal–Organic Coordination Networks at a Metal Surface

Alexandre Dmitriev, Hannes Spillmann, Nian Lin, Johannes V. Barth,* and Klaus Kern**

The construction of complex assemblies using molecular building blocks is paramount for the development of novel functional materials. A rich variety of molecular nanostructures and architectures with well-defined shapes and geometries have been obtained using transition-metal centers and concepts from coordination chemistry.[1–3] Metal–organic coordination networks (MOCNs) have been realized with specific topologies and a high structural stability.[4–12] MOCNs may exhibit intriguing properties, for example, molecular recognition, functionalities for heterogeneous asymmetric catalysis, and inclusion phenomena.[13–19] Moreover, for many applications the controlled nanoscale fabrication of functional molecular architectures at well-defined substrates is desirable.[20–22] However, most of the surface-supported assemblies reported to date are stabilized by relatively weak interactions, such as hydrogen bonding, van der Waals, or electrostatic forces, which implies a limited thermal stability.[23–25] Very recently, more robust one-dimensional (1D) nanostructures stabilized by metal–ligand interactions and the formation of metal–organic complexes at surfaces have been reported.[26–28]

Here we present a new strategy to fabricate surface-supported MOCNs at a well-defined metal surface under ultrahigh vacuum (UHV) conditions. The sequential deposition of 1,2,4-benzenetricarboxylic acid (trimellitic acid, tmla) molecules and Fe atoms on a clean Cu(100) substrate gives rise to the formation of 2D surface-supported open networks, stabilized by relatively strong lateral metal–organic coordination bonds. The MOCNs were investigated at the molecular level by scanning tunneling microscopy (STM). The precise control of the concentration ratio of the components allows for the assembly of distinct architectures. This approach opens up new possibilities for the bottom-up fabrication of low-dimensional functional materials.

The necessary precursors for surface-supported MOCNs are organic layers of a well-defined tmla phase, obtained by deposition of submonolayer tmla on the Cu(100) substrate. Figure 1 shows the corresponding well-ordered 2D domains, with a superstructure oriented along the Cu(100) high-symmetry directions. They extend over entire terraces and are commensurate with the underlying Cu substrate. The arrangement of the molecules is characterized by a [3 × 3] unit cell. A detailed experimental (using near-edge X-ray absorption fine structure spectroscopy (NEXAFS)) and theoretical (using density functional theory) analysis of this phase suggests that it consists of molecules with their aromatic ring slightly tilted out of the surface plane.[29] In view of the chemical reactivity of the substrate and the elevated temperature employed in the preparation,[29] it is expected that deprotonation of the carboxylic acid groups occurs, which is analogous to findings for other carboxylic acids on Cu surfaces under comparable conditions.[27–30] However, based on current experimental evidence, the intriguing possibility of an intramolecular hydrogen bond at the carboxylic groups in the *ortho* position of the adsorbed species cannot be ruled out. A further interesting feature of this phase is that it comprises homochiral domains, since the prochiral tmla molecules become chiral upon confinement to two dimensions, as discussed in more detail elsewhere.[29]

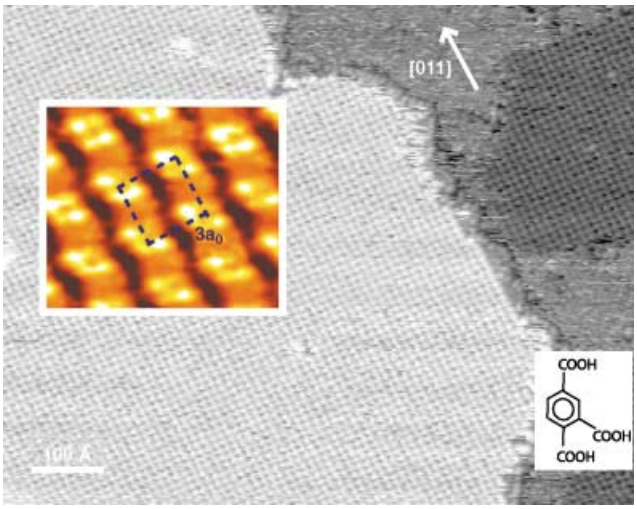

Figure 1. STM topography showing the 1,2,4-benzenetricarboxylic acid (tmla, shown bottom right) precursor layer deposited on a Cu(100) surface at 400 K. Domains comprising a commensurate regular structure of flat-lying molecules are resolved. The inset shows a high-resolution image with the [3 × 3] unit cell of the molecular layer. Individual tmla molecules are resolved as a four-lobe oval protrusion with a length of 8 Å.

Upon deposition of Fe atoms onto the tmla layer, the carboxylate groups readily react with the transition-metal adatoms. STM analysis (Figure 2a) reveals the formation of an extended regular network oriented along the principal directions of the substrate, at a coverage of one Fe atom to one tmla molecule. The network single domains are oriented along a substrate high-symmetry direction and are up to 100 × 100 nm in size, frequently covering entire substrate terraces (areas with compact islands, presumably from Fe aggregation, and other defects account for approximately 20 % of the total surface). The MOCN contains anisotropic cavities and can be found in two 90°-rotational domains, reflecting the symmetry of the substrate.

[*] Dr. N. Lin, Prof. Dr. K. Kern, A. Dmitriev, Dr. H. Spillmann
Max-Planck-Institut für Festkörperforschung
70569 Stuttgart (Germany)
Fax: (+49) 711-689-1079
E-mail: n.lin@fkf.mpg.de
k.kern@fkf.mpg.de
Dr. J. V. Barth, Prof. Dr. K. Kern
Institut de Physique des Nanostructures
Ecole Polytechnique Fédérale de Lausanne
1015 Lausanne (Switzerland)
E-mail: johannes.barth@epfl.ch

 © 2003 Wiley-VCH Verlag GmbH & Co. KGaA, Weinheim DOI: 10.1002/anie.200250610

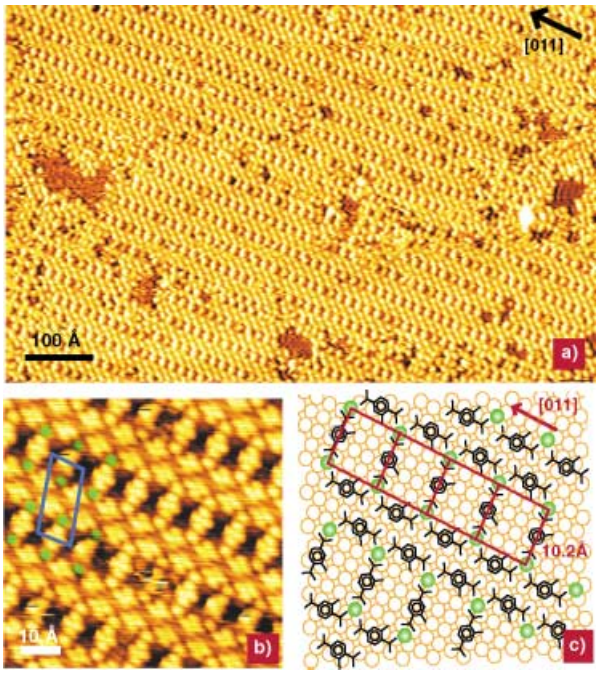

Figure 2. A "double-row MOCN" assembled by tuning the coverage ratio to one Fe atom per tmla molecule. a) Large-scale STM topography showing the regularly ordered network structure that comprises anisotropic cavities; b) high-resolution STM image revealing the four-lobe molecular structure. Single protrusions at the points of intersection throughout the network are associated with Fe atoms, laterally coordinated by tmla carboxylato moieties. The unit cell of the network is marked in blue and Fe atoms around are colored green; c) tentative model for the double-row Fe–carboxylate MOCN. The side carboxylate groups are assumed to be oriented perpendicular to the surface. Fe atoms (green) are arranged in a ladder-type structure with a 10.2×10.2 Å repeat unit.

High-resolution STM analysis (Figure 2b) allows individual tmla molecules to be distinguished; their characteristic four-lobe features are similar to the molecular resolution in the pure organic layer, which indicates that the flat adsorption geometry is preserved. Paired molecular rows running along the [011] direction have formed under the influence of the incorporated Fe atoms. The paired rows are interconnected by individual molecules oriented in the direction perpendicular to the rows. Thus this structure is designated "double-row MOCN". At the points of intersection bright protrusions are resolved, which are associated with the deposited Fe atoms, similar to the STM imaging of metal atoms in related compounds formed at the Cu(100) surface.[27,28] The relative orientation of the molecules with respect to the metal atoms indicates that the *para* carboxylate groups of tmla point towards the Fe atoms, which can be attributed to the formation of a lateral coordination bond. Consequently, the entire structure can be understood as an open-network-type Fe–carboxylate arrangement, stabilized by metal–ligand interactions.

A tentative geometrical model for the double-row MOCN based on an analysis of STM data is presented in Figure 2c. We assume that both Fe atoms and phenyl rings reside at the energetically preferential hollow sites of the substrate.[28,31] The Fe atoms in the double-row MOCN form ladders with a square $4a \times 4a$ repeat unit (the surface lattice parameter of Cu(100), $a = 2.55$ Å). Each Fe atom interacts with three tmla molecules: The data suggest that a unidentate linkage exists to the two neighboring molecules from the double row, along with a bidentate coupling to the isolated species in the perpendicular orientation. This arrangement implies a distorted fourfold coordination for each Fe atom, a configuration frequently encountered in 3D square-planar metal carboxylates.[32] However, it is important to note that with the present system the charge on both adsorbed tmla molecules and Fe atoms is strongly affected by the electrons of the metal surface, which effectively screen the adsorbate species and, in particular, prevent determination of the Fe oxidation state (for a more detailed discussion of this issue see Ref. [27]). In the model we assume that a too close distance of the laterally noncoordinated carboxylato groups at the *ortho* positions is avoided by their 90° rotation out of the surface plane. This behavior is suggested from a theoretical analysis of tmla bonding in the organic layer,[29] and is also a well-known conformational adaptation for carboxylic acids in solution chemistry. Furthermore the *ortho* side groups are placed randomly, since we found that they do not influence the primary frame structures of the MOCNs.[33] The effective cavity envelope is $\approx 3 \times 10$ Å, as estimated from high-resolution STM analysis. The stoichiometric Fe/tmla ratio in the model structure is determined to be 0.66, which falls below the necessary 1:1 ratio required for network formation.[34]

A second network type, designated "single-row MOCN", is obtained by increasing the adsorbate coverage ratio to two Fe atoms per tmla molecule. STM analysis (Figure 3a) shows that MOCNs with different topologies are formed. These MOCNs again follow the high-symmetry directions of the substrate and grow in extended islands. Two types of structures comprising different cavities can be discerned, which are designated the α and β phases, respectively. These structures always develop simultaneously, which signals that they are close in composition and energy. In the corresponding high-resolution STM data (Figure 3b,c) the positioning of the constituents is revealed. The networks consist of a sequential arrangement of individual tmla molecules and Fe atoms, which are identified by their respective imaging characteristics, similar to those in the double-row MOCN. In the α phase (Figure 3b) a rectangular unit cell and a cavity of similar shape and size as that in the double-row MOCN is identified. However, the cavity density is increased because the cavities in the α phase are separated by single tmla molecules, in contrast to the double-row structures where the cavities are separated by pairs of tmla molecules in one direction (Figure 2). Two 90° rotational domains are found in the α phase (inset, Figure 3a), which originate from its anisotropic shape. In the β phase (Figure 3c) a square unit cell comprising cavities of concave edges is found in a continuous 2D Fe–carboxylate network. The essential difference between the α and β phases is in the symmetry of the Fe–carboxylate linkage in the intersection points of the MOCNs. While it is always identical in the α phase, an alternating orientation of the Fe pairs at each intersection is found for the

 © 2003 Wiley-VCH Verlag GmbH & Co. KGaA, Weinheim

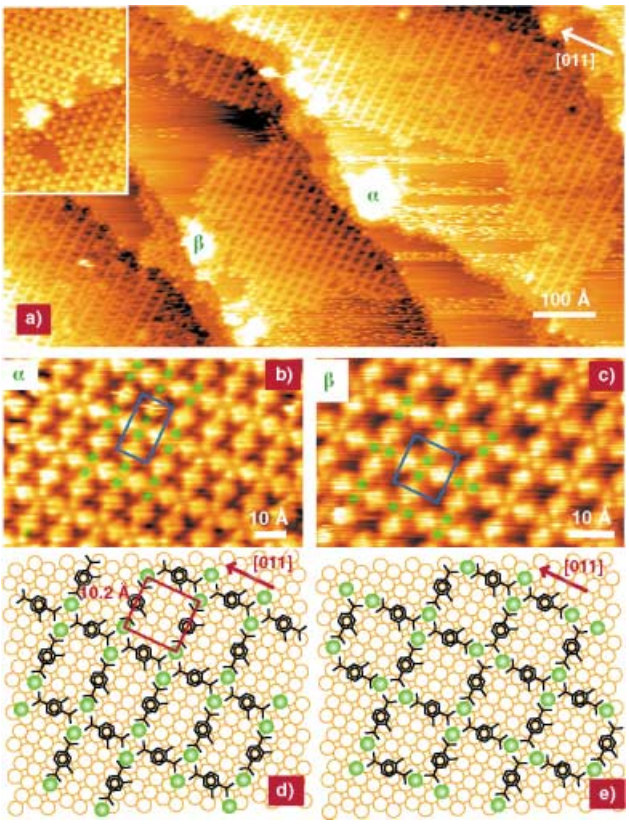

Figure 3. A "single-row MOCN" assembled by tuning the coverage ratio to two Fe atoms per tmla molecule. a) STM topography showing two species of regularly ordered networks, designated the α and β phases. In the inset, both 90°-rotational domains of the α phase are depicted; b,c) high-resolution STM images show that the detailed arrangement of Fe and tmla in both the α and β phases is resolved. A rectangular and square unit cell is characteristic for the networks of the α and β phases, respectively; d,e) tentative models that identify the α and β phases as MOCN isomers (coding as in Figure 2). Although both phases have the same stochiometry and contain Fe atoms with identical coordination environments, their geometrical arrangement is different.

β phase. This is illustrated by the corresponding models (Figure 3 d,e), which also show that the integral coordination of each Fe atom is equivalent for both phases. However, in the α phase a given tmla molecule has either two bidentate or four unidentate linkages to two Fe atoms, whereas in the β phase for every given molecule both bidentate and unidentate bonding are encountered at its extremities. Apparently the energy change associated with this subtle difference is small, which is understood as the reason for the simultaneous evolution of both phases under the employed conditions. Thus the two phases of the single-row MOCNs are closely related and can be regarded as structural isomers, which is a common finding for metal–organic frameworks.[10] In analogy with the double-row MOCN, the ideal 1:1 Fe/tmla stoichiometric coverage ratio for single-row MOCNs falls below the actual 2:1 value required for network formation.[34]

With the present system only the carboxylato groups in the *para* position seem to be integral for the formation and final topology of the encountered MOCNs, whereas the remaining side group is not directly involved in metal–organic complexation. Unfortunately the detailed positioning of side groups in the various network structures cannot be unambiguously determined by the STM data obtained, which is associated with the distortion of the molecules upon adsorption and the weak contribution of this moiety to the tunneling current. Note that the presence of the side group will nevertheless be important for the functionality of the cavity. For example, it may result in the formation of two mirror-symmetric MOCN cavities, since tmla is a 2D chiral species.

It is interesting to address the potential functionality of the obtained MOCNs. Firstly, the single- and double-row structures contain magnetic atoms which are periodically arranged. It is expected that the organic linkers mediate magnetic coupling between the Fe atoms, similar to effects in related metal–organic magnetic structures.[35,36] The ladder formations and 2D metal–organic linkages in the double-row and single-row MOCNs thus represent nanoscale magnetic arrangements with distinct symmetry. On the other hand, the obtained networks provide a regular arrangement of cavities with well-defined shape and chemistry. Finally, the MOCNs are of potential use as templates for 3D molecular architectures, such as nanoporous lattices.

In conclusion, we have succeeded in the rational design of 2D metal–organic networks, formed in situ under UHV conditions by sequential deposition of the organic linker molecule trimellitic acid and Fe atoms on a Cu(100) surface. The subtle variation of the relative quantities of the constituents that are deposited allows can steer the modular assembly of distinct metal–carboxylate network architectures. Our results indicate that, in general, 2D metal–organic coordination networks can be synthesized at well-defined surfaces. It is suggested that this approach opens novel avenues for the fabrication of nanoscale functional materials.

Experimental Section

Iron atoms and tmla molecules were co-deposited on the metal surface in a standard UHV chamber with a base pressure of $\sim 3 \times 10^{-10}$ mbar. A Cu(100) surface was prepared by repeated cycles of Ar^+ sputtering and subsequent annealing to 800 K, by which flat terraces of up to 50 nm width separated by monatomic steps were obtained. Tmla (99+ %, Sigma-Aldrich Chemie GmbH) was deposited by organic molecular beam epitaxy (OMBE) from a Knudsen-cell-type evaporator, held at 415 K during deposition. Fe atoms were evaporated using an electron-beam heating evaporator. To hinder Fe–Cu surface intermixing, which can be encountered in the pure Fe/Cu(100) system,[37] Fe was always deposited on an organic layer. Both tmla and Fe deposition were performed at a substrate temperature of 400 K to increase mobility and reactivity of the adsorbates and, thus, to allow for the formation of ordered structures. Coverages below full monolayer saturation were employed for the tmla precursor layers, in order to leave space for the formation of the more open network structures. STM experiments employing the constant-current mode were performed in situ following cooling to room temperature.

Received: November 22, 2002
Revised: March 12, 2003 [Z50610]

Keywords: coordination compounds · iron · nanomaterials · scanning tunneling microscopy · vacuum deposition

 © 2003 Wiley-VCH Verlag GmbH & Co. KGaA, Weinheim

[1] S. Leininger, B. Olenyuk, P. J. Stang, *Chem. Rev.* **2000**, *100*, 853.
[2] G. F. Swiegers, T. J. Malefetse, *Chem. Rev.* **2000**, *100*, 3483.
[3] B. J. Holliday, C. A. Mirkin, *Angew. Chem.* **2001**, *113*, 2076; *Angew. Chem. Int. Ed.* **2001**, *40*, 2022.
[4] J. Y. Lu, M. A. Lawandy, J. Li, T. Yuen, C. L. Lin, *Inorg. Chem.* **1999**, *38*, 2695.
[5] P. J. Stang, N. E. Persky, J. Manna, *J. Am. Chem. Soc.* **1997**, *119*, 4777.
[6] D. Venkataraman, G. B. Gardner, S. Lee, J. S. Moore, *J. Am. Chem. Soc.* **1995**, *117*, 11600.
[7] M. Fujita, Y. J. Kwon, S. Washizu, K. Ogura, *J. Am. Chem. Soc.* **1994**, *116*, 1151.
[8] L. R. MacGillivray, R. H. Groeneman, J. L. Atwood, *J. Am. Chem. Soc.* **1998**, *120*, 2676.
[9] S. R. Batten, R. Robson, *Angew. Chem.* **1998**, *110*, 1558; *Angew. Chem. Int. Ed.* **1998**, *37*, 1460.
[10] B. Moulton, M. J. Zaworotko, *Chem. Rev.* **2001**, *101*, 1629.
[11] M. Eddaoudi, D. B. Moler, H. Li, B. Chen, T. M. Reineke, M. O'Keeffe, O. M. Yaghi, *Acc. Chem. Res.* **2001**, *34*, 319.
[12] Y. Cui, O. R. Evans, H. L. Ngo, P. S. White, W. Lin, *Angew. Chem. Int. Ed.* **2002**, *114*, 1207; *Angew. Chem. Int. Ed.* **2002**, *41*, 1159.
[13] H. Li, M. Eddaoudi, M. O'Keeffe, O. M. Yaghi, *Nature* **1999**, *402*, 276.
[14] J. S. Seo, D. Whang, H. Lee, S. I. Jun, J. Oh, Y. J. Jeon, K. Kim, *Nature* **2000**, *404*, 982.
[15] G. B. Gardner, D. Venkataraman, J. S. Moore, S. Lee, *Nature* **1995**, *374*, 792.
[16] O. M. Yaghi, G. Li, H. Li, *Nature* **1995**, *378*, 703.
[17] S. S.-Y. Chui, S. M.-F. Lo, J. P. H. Charmant, A. G. Orpen, I. D. Williams, *Science* **1999**, *283*, 1148.
[18] B. Chen, M. Eddaoudi, S. T. Hyde, M. O'Keeffe, O. M. Yaghi, *Science* **2001**, *291*, 102.
[19] C. J. Kepert, T. J. Prior, M. J. Rosseinsky, *J. Am. Chem. Soc.* **2000**, *122*, 5158.
[20] C. P. Collier, E. W. Wong, M. Belohradský, F. M. Raymo, J. F. Stoddart, P. J. Kuekes, R. S. Williams, J. R. Heath, *Science* **1999**, *285*, 391.
[21] G. P. Lopinski, D. D. M. Wayner, R. A. Wolkow, *Nature* **2000**, *406*, 48.
[22] C. Joachim, J. K. Gimzewski, A. Aviram, *Nature* **2000**, *408*, 541.
[23] T. Yokoyama, S. Yokoyama, T. Kamikado, Y. Okuno, S. Mashiko, *Nature* **2001**, *413*, 619.
[24] J. V. Barth, J. Weckesser, C. Cai, P. Günter, L. Bürgi, O. Jeandupeux, K. Kern, *Angew. Chem.* **2000**, *112*, 1285; *Angew. Chem. Int. Ed.* **2000**, *39*, 1230; J. V. Barth, J. Weckesser, G. Trimarchi, M. Vladimirova, A. De Vita, C. Cai, H. Brune, P. Günter, K. Kern, *J. Am. Chem. Soc.* **2002**, *124*, 7991.
[25] M. Böhringer, K. Morgenstern, W.-D. Schneider, R. Berndt, F. Mauri, A. De Vita, R. Car, *Phys. Rev. Lett.* **1999**, *83*, 324.
[26] D. G. Kurth, N. Severin, J. P. Rabe, *Angew. Chem.* **2002**, *114*, 3833; *Angew. Chem. Int. Ed.* **2002**, *41*, 3681.
[27] N. Lin, A. Dmitriev, J. Weckesser, J. V. Barth, K. Kern, *Angew. Chem.* **2002**, *114*, 4973; *Angew. Chem. Int. Ed.* **2002**, *41*, 4779.
[28] P. Messina, A. Dmitriev, N. Lin, H. Spillmann, M. Abel, J. V. Barth, K. Kern, *J. Am. Chem. Soc.* **2002**, *124*, 14000.
[29] A. Dmitriev, H. Spillmann, N. Lin, P. Messina, M. Abel, A. Seitsonen, M. Parrinello, J. V. Barth, K. Kern, unpublished results **2002**.
[30] C. C. Perry, S. Haq, B. G. Frederick, N. V. Richardson, *Surf. Sci.* **1998**, *409*, 512.
[31] A. Dmitriev, N. Lin, J. Weckesser, J. V. Barth, K. Kern, *J. Phys. Chem. B* **2002**, *106*, 6907.
[32] R. C. Mehrotra, R. Bohra, *Metal Carboxylates*, Academic Press, London, **1983**.
[33] In fact, by using 1,4-benzenedicarboxylic acid (terephtalic acid, TPA), a molecule with two carboxylic groups at *para* positions, exactly the same MOCN structures can be fabricated, which proves that the side group does not play a significant role in the MOCN formation.
[34] This difference is attributed to the effective loss of Fe atoms in other surface chemical processes, that is, the entire amount of deposited Fe is not employed in coordination network formation. Decoration of substrate step edges, and in particular Fe island formation are frequently suggested from inspection of STM topographs. In addition, a small percentage of the Fe atoms might be lost in substrate atom-exchange processes.
[35] E. Breuning, M. Ruben, J.-M. Lehn, F. Renz, Y. Garcia, V. Ksenofontov, P. Gütlich, E. Wegelius, K. Rissanen, *Angew. Chem.* **2000**, *112*, 2563; *Angew. Chem. Int. Ed.* **2000**, *39*, 2504.
[36] B. Moulton, J. Lu, R. Hajndl, S. Hariharan, M. J. Zaworotko, *Angew. Chem.* **2002**, *114*, 2945; *Angew. Chem. Int. Ed.* **2002**, *41*, 2821.
[37] D. D. Chambliss, K. E. Johnson, *Phys. Rev. B* **1994**, *50*, 5012.

 © 2003 Wiley-VCH Verlag GmbH & Co. KGaA, Weinheim